

1 **The ant fungus garden acts as an external digestive system**

2 **Authors:** Andrés Mauricio Caraballo-Rodríguez¹, Sara P. Puckett², Kathleen E. Kyle³, Daniel Petras^{1,4},
3 Ricardo da Silva⁵, Louis-Félix Nothias¹, Madeleine Ernst⁶, Justin J.J. van der Hooft⁷, Anupriya Tripathi^{1,8,9},
4 Mingxun Wang^{1,10}, Marcy J. Balunas², Jonathan L. Klassen^{3**}, Pieter C. Dorrestein^{1*}

5 **Affiliations**

6 ¹ Collaborative Mass Spectrometry Innovation Center, Skaggs School of Pharmacy and Pharmaceutical
7 Sciences, University of California San Diego, La Jolla, CA.

8 ² Division of Medicinal Chemistry, Department of Pharmaceutical Sciences, University of Connecticut,
9 Storrs, CT 06269, USA.

10 ³ Department of Molecular and Cell Biology, University of Connecticut, Storrs, CT, USA.

11 ⁴ Scripps Institution of Oceanography, University of California San Diego, La Jolla, CA

12 ⁵ School of Pharmaceutical Sciences of Ribeirão Preto, University of São Paulo, Ribeirão Preto, SP, Brazil.

13 ⁶ Section for Clinical Mass Spectrometry, Danish Center for Neonatal Screening, Department of Congenital
14 Disorders, Statens Serum Institut, Copenhagen, Denmark

15 ⁷ Bioinformatics Group, Wageningen University, 6708 PB, Wageningen, the Netherlands.

16 ⁸ Division of Biological Sciences, University of California—San Diego, San Diego, California, USA

17 ⁹ Department of Pediatrics, University of California—San Diego, San Diego, California, USA

18 ¹⁰ Ometa Labs LLC

19 * to whom correspondence should be addressed for the mass spectrometry and data analysis:
20 pdorrestein@ucsd.edu. ** to whom correspondence should be addressed regarding the ant-fungus
21 system: jonathan.klassen@uconn.edu.

22 **Contributions**

23 PCD and AMCR created the concept of applying 3D cartography to fungus gardens. DP conceived the
24 idea of chemical proportionality. KEK, SPP and AMCR deconstructed fungus gardens and prepared
25 extracts. AMCR processed samples for LC-MS/MS acquisition. KEK and JLK collected and maintained ant
26 colonies. AMCR, DP, RS, ME, JJJvdH and PCD performed data analysis. LFN supported FBMN. LFN and AT
27 supported molecular formula assignment and structure prediction workflows in the GNPS environment.
28 MW supported FBMN and data visualization from GNPS. PCD, JLK and MJB provided supervision and

29 funding for the project. AMCR, JLK and PCD wrote the manuscript. All authors contributed to the writing
30 and editing of the manuscript.

31 **Abstract**

32 Most animals digest their food within their own bodies, but some do not. Many species of ants grow
33 fungus gardens that pre-digest food as an essential step of the ants' nutrient uptake. To better
34 understand this digestion process, we generated a 3D molecular map of an *Atta texana* fungus garden,
35 revealing chemical modifications mediated by the fungus garden as plant material passes through.

36 **Main**

37 Many ant species access plant-derived nutrients with the help of fungal symbionts.¹ For
38 example, leaf-cutter ants grow a specific cultivar fungus in specialized underground structures called
39 "fungus gardens" as their main food source. This cultivar fungus breaks down forage material such as
40 leaves provided by the ants to obtain the necessary nutrients for its own growth.² In turn, the ants eat
41 the fungus' specialized hyphal tips, known as gongylidia, which contain nutrients that are metabolically
42 available to the ants.³ Fungal enzymes present in the garden transform plant metabolites such as
43 polysaccharides and phenolic compounds.⁴⁻⁶ Fungus gardens from leaf-cutter ants have been described
44 as bioreactors due to their capacity to process plant constituents that provide small carbohydrates.⁶
45 Primary metabolites have been measured in the fungus gardens, and correlated to the differential
46 distribution of fungal metabolic enzymes.^{2,7} Nonetheless, maps of metabolic diversity in ant fungus
47 gardens have remained unavailable due to the lack of computational workflows that go beyond the
48 analysis of a few selected metabolites, which did not exist until recently.

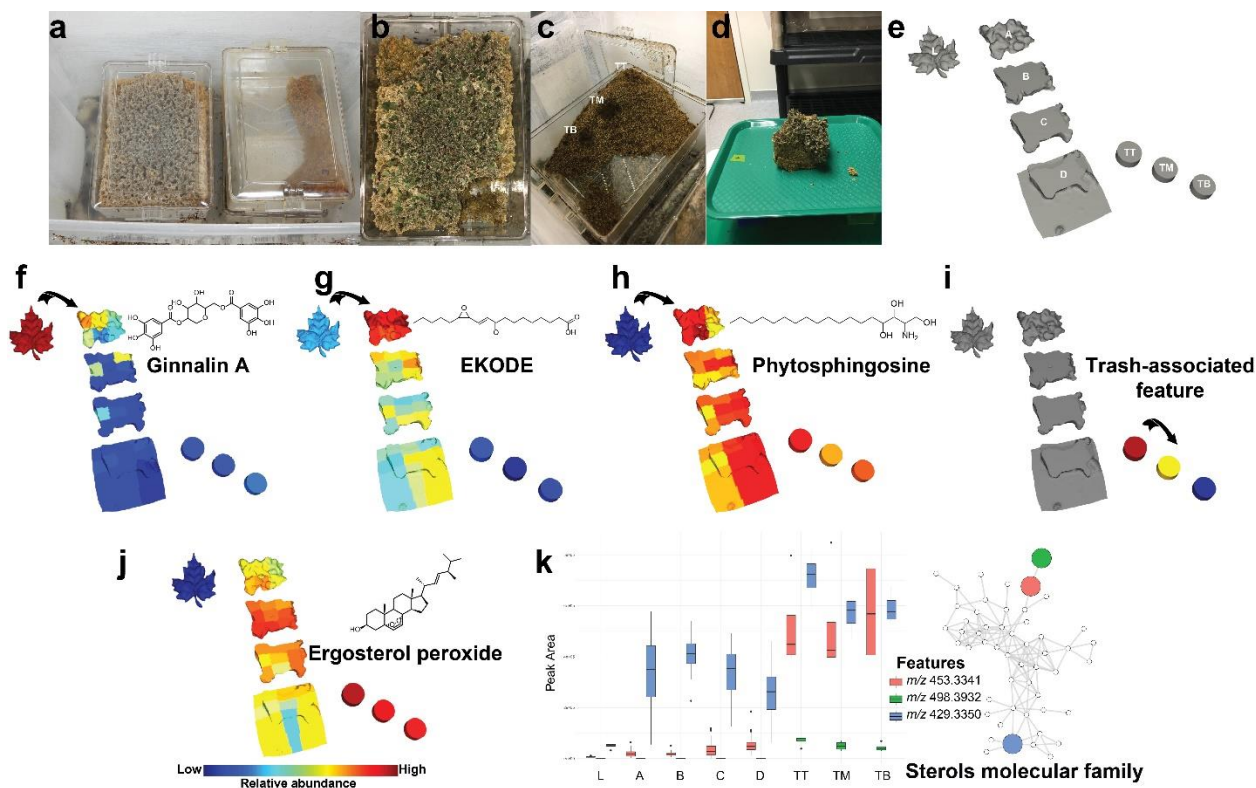
49 Here, we highlight chemical transformations in a laboratory maintained *Atta texana* fungus
50 garden using molecular networking,⁸⁻¹⁰ 3D cartography,¹¹ and meta mass-shift analysis¹². The use of
51 non-targeted metabolomics, via liquid chromatography - tandem mass spectrometry (LC-MS/MS),^{10,13-15}
52 enabled us to identify molecular families and metabolite features (**Supplementary Fig. S1-S2**) that

53 chemically differentiate plant materials that are sequentially consumed by the fungus as they pass through
54 the garden (**Supplementary Fig. S3-S4**). These molecular families were annotated using various
55 annotation tools combined using the MolNetEnhancer^{10,16} workflow resulting in the annotation of plant
56 and fungus related chemical compound classes. Furthermore, we identified the types of chemical
57 transformations that are carried out based on the differential abundance of compounds that occur
58 among the sampled layers of the fungus garden (**Online methods**). The observed transformations
59 provide insight into the chemistry and the modification of molecules (representing potential chemical
60 transformations or differential degradation) inside an ant fungus garden.

61 After plant materials are incorporated into the fungus garden by the ants, they are further
62 processed by the fungus, and following digestion any recalcitrant plant biomass becomes trash that the
63 ants remove from the garden (**Fig. 1**). Molecules from the plant material, such as saccharide-decorated
64 flavonoids and phenolic compounds, decreased in relative abundance when moving from the top to the
65 bottom of the fungus garden, in contrast to other compounds that increased in relative abundance
66 across these layers (**Supplementary Fig. S3**), either due to chemical modifications or preferential
67 degradation of the less abundant compound (**Supplementary Fig. S5-S14**). Fungus garden and trash
68 samples were enriched with phytosphingosines (**Supplementary Fig. S9**), whereas features associated
69 with the trash material were enriched in steroids (**Fig. 1, Supplementary Fig. S10**), such as the fungal
70 metabolite ergosterol peroxide,^{17,18} and oxylipins (**Supplementary Fig. S11-S12**). Gradients of other
71 plant-derived metabolite abundances, such as triterpenoid derivatives, were observed as we moved
72 from the top to the bottom of the fungus garden, leading to high abundances at the bottom of the
73 fungus garden and in the trash (**Supplementary Fig. S13-S14**). These gradients parallel the metabolic
74 transformations of food components in the digestive tract of animals, such as those involving the
75 metabolism of flavonoids, steroids (molecules with steroidal cores), and fatty acids.¹⁹⁻²¹ In a similar way
76 to how food changes during its transit through the digestive tract of animals and the residual material is

77 discarded, plant material is transformed in the fungus garden and, finally, the residual material is
78 removed from the colony. Thus, the initial food material is chemically distinct when compared to the
79 trash material removed by the ants (**Supplementary Fig. S4**).

80 Digestive processes generate modified products whose precursors are consumed. To provide an
81 overview of putative metabolic transformations occurring in ants' fungus gardens, we combined mass
82 shift analysis¹² and discovered relative metabolite abundances for pairs from each section of the fungus
83 garden by calculating a proportionality score (**Online Methods**). By considering the proportion between
84 the relative abundances of two chemically related molecules (i.e. connected nodes in a network), their
85 mass shifts and the modifications that these imply (e.g. a 15.996 Da shift indicates a gain or loss of
86 oxygen, 2.015 Da an oxidation or reduction through the loss or addition of H₂), and their distribution
87 between two locations (leaves, layers of fungus garden and layers of trash material) we can discover
88 related molecules that have the largest variance in abundance between the layers (**Online Methods, Fig.**
89 **1-3; Supplementary Fig. S15-S17**). It should be noted that this approach cannot differentiate between
90 different types of changes in the absolute abundance of each molecule, e.g., chemical transformation
91 leading to the accumulation of a molecule or the complete degradation of a molecule leading to its
92 decreased abundance. However, by considering the chemical similarities and relative abundances
93 between each molecular pair that are identified by molecular networking we imply relationships
94 between these molecules that are consistent with each molecule belonging to the same structural class
95 and their abundance changes across samples. We interpret the abundance changes across layers to be
96 largely driven by anabolic or catabolic pathways, potentially linked to enzymatically mediated
97 transformations. Absolute molecular concentrations might also be altered by additions from the
98 external environment, but the closed nature of the laboratory maintained ant fungus gardens means
99 that such additions essentially only occur directionally via the leaves when they are incorporated into
100 the fungus garden by the ants.



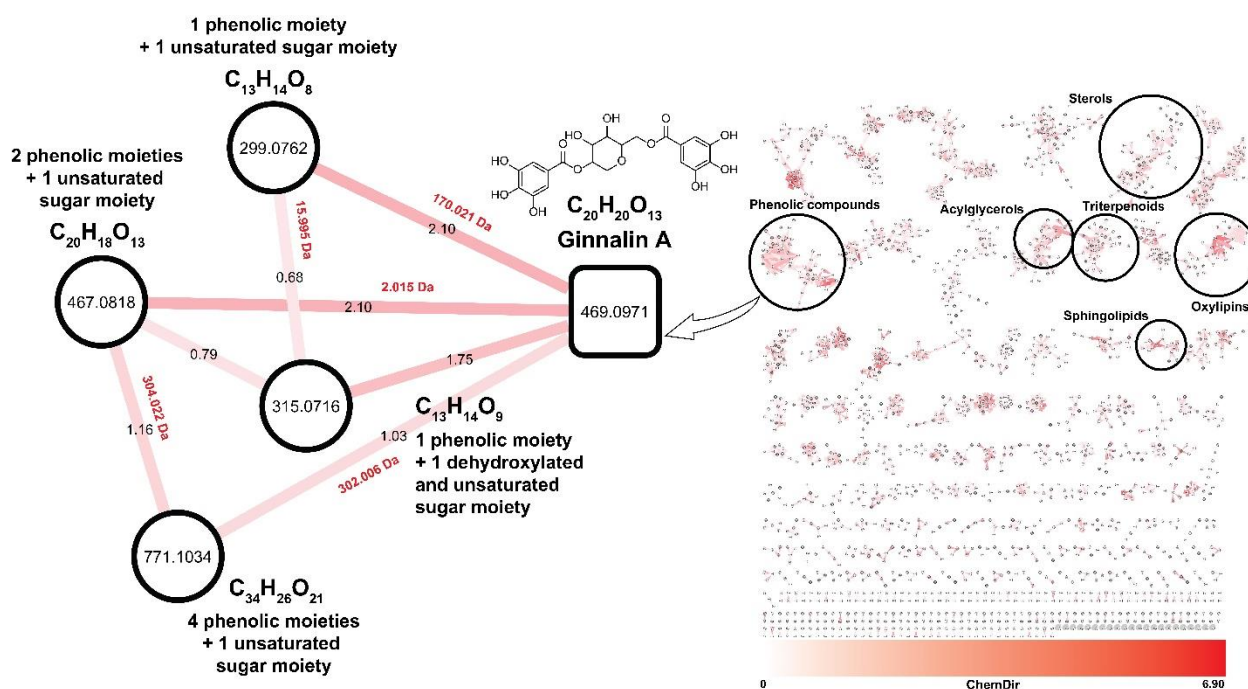
101 **Fig. 1 | Spatial distribution of molecular signatures from *A. texana* fungus garden.** a-d. Deconstruction of the *Atta texana*
 102 JKH000189 fungus garden: a. Plastic containers with an *Atta texana* fungus garden (left) and waste material removed by ants
 103 (right). Ants have free access to both chambers; b. This picture shows the location of a removed 10x10x10cm portion of the
 104 fungus garden (lower right corner). The green fragments at the top of the fungus garden are freshly incorporated maple leaves;
 105 c. Chamber containing the trash material removed from the fungus garden by the ants. Three sampling locations from the trash
 106 are highlighted as “TB”, “TM”, and “TT”; d. Removed 10x10x10cm fungus garden portion for consequent sample preparation
 107 for LC-MS/MS; e. 3D representation of deconstructed fungus garden portion, as shown in (d). On the left side, a representation
 108 of the maple leaves (L) placed in the outer colony box that ants cut and incorporate into the top of the fungus garden; layers of
 109 the fungus garden from top to bottom (A, B, C, and D) and at the right side of the figure, the representation of the three sample
 110 locations from the trash chamber, from top to bottom (TT, TM and TB); f-i. Spatial distribution of ginnalin A, detected as m/z
 111 469.0971 (f), (E)-9-oxo-11-(3-pentylloxiran-2-yl)undec-10-enoic acid (trans-EKODE-(E)-Ib) detected as m/z 311.221 (g),
 112 phytosphingosine detected as m/z 318.2995 (h), unknown feature associated to the trash material detected as m/z 474.3783
 113 (i); j-k. The abundance of features belonging to the molecular family of sterols were also detected at high intensity in the trash
 114 material, suggesting that these compounds accumulate in the trash material: j. Ergosterol peroxide detected as m/z 429.3350;
 115 k. Abundance of features associated with trash material belonging to the sterols molecular family (ergosterol peroxide, feature
 116 m/z 498.3932 and feature m/z 453.3341). The boxes represent the 25%, 50%, and 75% quantile and the whiskers extend ± 1.5
 117 times the interquartile range. The annotation of ergosterol peroxide from GNPS libraries (cosine score = 0.71) was confirmed
 118 using a reference standard (Supplementary Table S1), a level 1 match according to the 2007 metabolomics initiative,³² while
 119 the m/z 498.3932 is consistent with a molecular formula of $C_{32}H_{52}NO_3$ (error 1.9 ppm) and belongs to the same molecular
 120 family - a level 3 match.³² A detailed description of the sample preparation can be found in the **Online methods**. See **online**

121 **methods** for more details and a molecular cartography of this deconstructed *Atta texana* fungus garden visualized in 'ili¹¹ is
122 shown in **Supplementary Movie S1** [[https://youtu.be/ ikhKelfrY8](https://youtu.be/ikhKelfrY8)].

123 In this study, we introduce the proportionality concept using a modification to Meta-Mass Shift
124 analysis,¹² by considering also the abundances of the detected molecules, to quickly highlight features
125 (metabolites) potentially involved in chemical transformations. Proportionality scores highlighted such
126 changing pairs of nodes occurring in various locations in the *A. texana* fungus garden, and the associated
127 mass shifts provided evidence of the types of modifications occurring in the sampled locations (**Fig. 2**).
128 Proportionality scoring is a logarithmic expression, and we selected an absolute value of 1 as cutoff to
129 prioritize potential transformations because a score close to zero will indicate a low ratio of
130 abundances between two chemically related molecules in two sample locations, suggesting a low
131 change of intensities between the two mass spectrometry features of the molecular network pair (see
132 the definition and calculation of the proportionality scores in **Online Methods**). Differences representing
133 a gain or loss of H₂ (2.015 Da) were the predominant type of chemical transformation observed
134 throughout the entire data set, being one of the most frequent mass shifts with a proportionality score >
135 1 among leaves, the fungus garden and trash layers (**Fig. 3**). This common modification was observed in
136 molecular families such as phenolic compounds (**Fig. 2**) and phytosphingosines (**Supplementary Fig.**
137 **S9**).²² Mass shifts corresponding to CH₂ (14.015 Da) and C₂H₄ (28.031 Da) were other common changes
138 observed in the top layer of the fungus garden, as well as between the bottom layer of the fungus
139 garden and the trash (**Fig. 3**). Oxidation or dehydroxylation combined with reduction processes result in
140 the gain or loss of oxygen that can be detected and a mass difference of 15.995 Da. The transformations
141 corresponding to these differences were more frequently observed at the top layer of the fungus garden
142 during the breakdown of flavonoids and phenolic compounds (**Fig. 3, Supplementary Fig. S5-S8**).

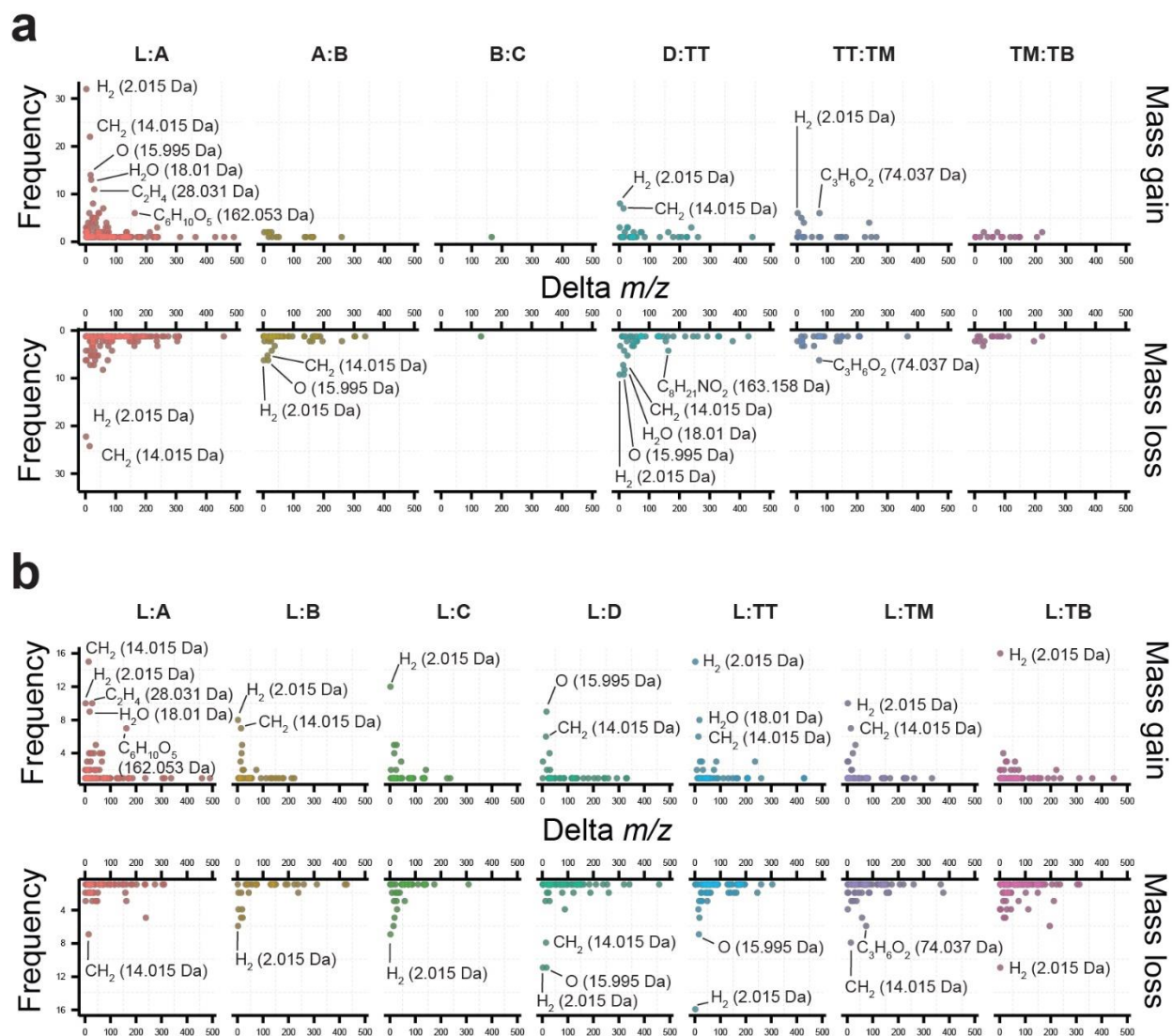
143 Chemical transformations consistent with addition or removal of sugar moieties in the *A. texana*
144 fungus garden were also highlighted by proportionality scores > 1. These transformations,

145 corresponding to mass differences of 162.053 Da ($C_6H_{10}O_5$), were associated with plant material and the
146 top layers of the fungus garden (**Fig. 3**), and corresponded to transformations involving chemical
147 substructures that were present in plant metabolites such as flavonoids and acylglycerols
148 (**Supplementary Fig. S6, S17**). The mass difference of 162.053 Da, consistent with the gain or loss of a
149 sugar moiety, was also present in a molecular family of acylglycerols and occurred in the top layer of the
150 fungus garden (**Supplementary Fig. S17**).



151 **Fig. 2 | Potential transformations highlighted by the proportional scoring of untargeted metabolomics data from *Atta texana***
152 **fungus garden.** Chemical features are highlighted from a molecular network based on their high proportionality score
153 calculated throughout the sample types from leaves, fungus garden layers and trash layers (red edge with label indicating the
154 proportionality score). The feature corresponding to m/z 469.0971 annotated as ginnalin A, a bioactive phenolic compound,²⁵
155 was identified as a potential partner in several chemical transformations. Based on the information regarding the mass shifts
156 (red labels, in Daltons) of the connected nodes, and the suggested molecular formula, putative structures can be suggested
157 based on their fragmentation patterns. Together, with the spatial distribution (**Supplementary Figures S8 and S16**), it can be
158 suggested the involvement of this molecular family in chemical transformations occurring in the fungus garden. Ginnalin A was
159 detected in the leaves as well as in the fungus garden while the features of m/z 299.0762 and m/z 467.0818 were only detected
160 in the plant material. This suggest that ginnalin A and related features, m/z 315.0717 and m/z 771.1034 might be either
161 transformed from m/z 467.0818 and m/z 299.0762, which reach undetectable levels in the fungus garden, or are more

162 recalcitrant to degradation. Similarities in the fragmentation spectra (MS/MS) of these compounds enabled us to gain insight
 163 into their potential structural differences. All fragmentation spectra for the connected nodes in the molecular network shown
 164 in the figure shared the m/z 153.02 base peak corresponding to the phenolic moiety (gallic acid), indicating an unsaturation
 165 located in the sugar moiety. The identification of ginnalin A based on spectral similarity to GNPS libraries (cosine score = 0.95)
 166 corresponds to annotation at level 2 according to the 2007 metabolomics standards initiative,²⁶ while the matches for the
 167 related molecules shown are at the molecular family level, a level 3 annotation.²⁶ Although double bonds of the saccharide
 168 moiety can be suggested based on the molecular formula, it is not possible to define their location or the stereochemistry
 169 thereof without additional information. Other examples of potential chemical transformations in *Atta texana* fungus gardens
 170 described using this proportionality approach can be found in **Supplementary Fig. S15-S17**.



171 **Fig. 3 |** Frequency of delta masses observed in metabolomics data from a deconstructed *Atta texana* fungus garden.

172 Proportionality metrics were calculated between compounds found in different layers of the fungus garden, as well as between
 173 plant, fungus garden and trash material: **a**. Frequency of delta masses calculated between samples corresponding to leaves (L),
 174 layers of fungus garden from top to bottom (A, B, C and D), and trash material (samples collected from the chamber that ants

175 use to deposit the trash material. From the top, TT; middle, TM and bottom, TB). **b.** Frequency of delta masses between
176 compounds found in leaves (L) and each of the fungus garden and trash layers. Mass shifts between network pairs with
177 proportionality scores > 1 were retrieved as indicative of chemical transformations prevalent in specific locations. Frequencies
178 of annotated mass shifts observed from network pairs with high proportionality scores (proportionality values > 1, See
179 [Supplementary Table S4](#)) indicated that the regions where most transformations occur are between leaves and the top layer of
180 fungus garden (Layer A), between the bottom of fungus garden (Layer D) and the trash, as well as between the trash layers (TT,
181 TM and TB). None of the observed mass shifts resulted in a high score when proportionality was calculated between fungus
182 layers C and D (proportionality C:D). The figure in panel **b** shows the most frequent mass shifts observed from network pairs
183 with highest transformation rates from proportionality calculated between leaves (L) and each of the sample groups, fungus
184 garden and trash layers. This indicates that most of these transformations are still observed throughout the fungus garden but
185 also that some of them are specific to the trash, such as $C_8H_{21}NO_2$ (163.158 Da) (as observed in panel **a**).

186 The existence of chemical gradients in the fungus garden resembles a digestion process, with
187 substrates being modified to facilitate their consumption and generating residues that need to be
188 removed or discarded, as shown here by plant constituents passing through an ant-fungus garden
189 ecosystem. The metabolic transformations observed here are consistent with the modification of lipids
190 by fungus gardens, as well as plant volatile compounds by fungus-garden-associated bacteria, as
191 recently reported from leaf-cutter ant fungus gardens,^{23,24} adding further support to the model
192 describing fungus gardens as external digestive systems for ants. The chemical modifications and the
193 types of (bio)transformations observed in our study might not vary based on changes in the available
194 plant material, although environmental factors such as temperature or humidity, and the composition of
195 microbiome that are associated with ants and their fungus gardens,²³ will likely influence these
196 modifications.

197 In summary, the 3D cartographic analyses performed in this study provide an overview of
198 chemical changes occurring in a fungus garden. Our results demonstrate that chemical transformations
199 of the plant components are associated with certain regions of the fungus garden and show that the
200 degree of modifications are more extensive than previously described.^{24,25} The results further support a
201 model where fungus gardens serve a similar function to the mammalian digestive tract, where its
202 function is to gradually metabolize food molecules from top to bottom akin to the gastrointestinal tract

203 from the mouth to anus. In other words, the plant material is digested starting when leaves enter the
204 fungus garden, and continues all the way through the bottom layer of the fungus garden. Finally, there
205 are molecules that are removed from the system into the fungus garden trash. This is reminiscent of a
206 food to digestive tract to feces scheme.²¹ How the food molecules move down the ant's external
207 digestive tract is not yet known, but the ants "clean up" after themselves via removal of unwanted
208 fungal garden parts to the trash. The methodologies that we used provide a complementary overview of
209 metabolic processes occurring in a laboratory maintained *A. texana* fungus garden and we expect the
210 approach can be leveraged to unravel similar processes in natural environments to compare between
211 natural and lab-maintained ecosystems.

212 **Online content**

213 Methods, additional references, Nature Research reporting summaries, source data, statements of data
214 availability and associated accession codes are available on line.

215 **Acknowledgements.** AMCR and PCD were supported by the National Sciences Foundation grant IOS-
216 1656481. KEK, SPP, JLK and MJB were supported by NSF grant IOS-1656475. DP was supported by the
217 Deutsche Forschungsgemeinschaft (DFG) with grant PE 2600/1. RRdS was supported by the São Paulo
218 Research Foundation (Awards FAPESP 2017/18922–2 and 2019/05026–4). PCD was supported by the
219 Gordon and Betty Moore Foundation through Grant GBMF7622, the U.S. National Institutes of Health
220 for the Center (P41 GM103484, R03 CA211211, R01 GM107550). LFN was supported by the U.S.
221 National Institutes of Health (R01 GM107550). JJvdH was supported by an ASDI eScience grant,
222 ASDI.2017.030, from the Netherlands eScience Center — NLeSC. We thank Alan K. Jarmusch for his
223 valuable comments in earlier versions of the manuscript.

224 **Competing interests** PCD is a scientific advisor to Sirenas. MW is Founder of Ometa Labs LLC.

225 **References**

- 226 1. Currie, C. R. A Community of Ants, Fungi, and Bacteria: A Multilateral Approach to Studying Symbiosis. *Annu. Rev.*
227 *Microbiol.* **55**, 357–380 (2001).

- 228 2. Lange, L. & Grell, M. N. The prominent role of fungi and fungal enzymes in the ant–fungus biomass conversion symbiosis.
229 *Appl. Microbiol. Biotechnol.* **98**, 4839–4851 (2014).
- 230 3. De Fine Licht, H. H., Boomsma, J. J. & Tunlid, A. Symbiotic adaptations in the fungal cultivar of leaf-cutting ants. *Nat.*
231 *Commun.* **5**, 5675 (2014).
- 232 4. Richard, F.-J., Mora, P., Errard, C. & Rouland, C. Digestive capacities of leaf-cutting ants and the contribution of their fungal
233 cultivar to the degradation of plant material. *J Comp Physiol B* **175**, 297–303 (2005).
- 234 5. De Fine Licht, H. H. *et al.* Laccase detoxification mediates the nutritional alliance between leaf-cutting ants and fungus-
235 garden symbionts. *Proc Natl Acad Sci U A* **110**, 583–587 (2013).
- 236 6. Somera, A. F., Lima, A. M., Dos Santos-Neto, Á. J., Lanças, F. M. & Bacci, M., Jr. Leaf-cutter ant fungus gardens are biphasic
237 mixed microbial bioreactors that convert plant biomass to polyols with biotechnological applications. *Appl Env. Microbiol*
238 **81**, 4525–4535 (2015).
- 239 7. Huang, E. L. *et al.* The fungus gardens of leaf-cutter ants undergo a distinct physiological transition during biomass
240 degradation. *Environ. Microbiol. Rep.* **6**, 389–395 (2014).
- 241 8. Watrous, J. *et al.* Mass spectral molecular networking of living microbial colonies. *Proc Natl Acad Sci U A* **109**, E1743-52
242 (2012).
- 243 9. Wang, M. *et al.* Sharing and community curation of mass spectrometry data with Global Natural Products Social Molecular
244 Networking. *Nat Biotechnol* **34**, 828–837 (2016).
- 245 10. Ernst, M. *et al.* MolNetEnhancer: Enhanced Molecular Networks by Integrating Metabolome Mining and Annotation Tools.
246 *Metabolites* **9**, (2019).
- 247 11. Protsyuk, I. *et al.* 3D molecular cartography using LC-MS facilitated by Optimus and 'ili software. *Nat Protoc* **13**, 134–154
248 (2018).
- 249 12. Hartmann, A. C. *et al.* Meta-mass shift chemical profiling of metabolomes from coral reefs. *Proc Natl Acad Sci U A* **114**,
250 11685–11690 (2017).
- 251 13. Mohimani, H. *et al.* Dereplication of peptidic natural products through database search of mass spectra. *Nat Chem Biol* **13**,
252 30–37 (2017).
- 253 14. da Silva, R. R. *et al.* Propagating annotations of molecular networks using in silico fragmentation. *PLoS Comput Biol* **14**,
254 e1006089 (2018).
- 255 15. Hooft, J. J. J. van der, Wandy, J., Barrett, M. P., Burgess, K. E. V. & Rogers, S. Topic modeling for untargeted substructure
256 exploration in metabolomics. *Proc. Natl. Acad. Sci.* **113**, 13738–13743 (2016).

- 257 16. Djombou Feunang, Y. *et al.* ClassyFire: automated chemical classification with a comprehensive, computable taxonomy. *J*
258 *Cheminform* **8**, 61 (2016).
- 259 17. Krzyczkowski, W. *et al.* Isolation and quantitative determination of ergosterol peroxide in various edible mushroom
260 species. *Food Chem* **113**, 351–355 (2009).
- 261 18. Nowak, R. *et al.* A New Method for the Isolation of Ergosterol and Peroxyergosterol as Active Compounds of
262 *Hygrophoropsis aurantiaca* and in Vitro Antiproliferative Activity of Isolated Ergosterol Peroxide. *Molecules* **21**, (2016).
- 263 19. Cant, J. P., McBride, B. W. & Croom, W. J., Jr. The regulation of intestinal metabolism and its impact on whole animal
264 energetics. *J Anim Sci* **74**, 2541–2553 (1996).
- 265 20. Novais, F. J. *et al.* Identification of a metabolomic signature associated with feed efficiency in beef cattle. *BMC Genomics*
266 **20**, 8 (2019).
- 267 21. Quinn, R. A. *et al.* Global chemical effects of the microbiome include new bile-acid conjugations. *Nature* **579**, 123–129
268 (2020).
- 269 22. Kondo, N. *et al.* Identification of the phytosphingosine metabolic pathway leading to odd-numbered fatty acids. *Nat*
270 *Commun* **5**, 5338 (2014).
- 271 23. Francoeur, C. B. *et al.* Bacteria Contribute to Plant Secondary Compound Degradation in a Generalist Herbivore System.
272 *mBio* **11**, (2020).
- 273 24. Khadempour, L. *et al.* From plants to ants: Fungal modification of leaf lipids for nutrition and communication in the leaf-
274 cutter ant fungal garden ecosystem. *bioRxiv* 2020.07.28.224139 (2020) doi:10.1101/2020.07.28.224139.
- 275 25. Khadempour, L. *et al.* The fungal cultivar of leaf-cutter ants produces specific enzymes in response to different plant
276 substrates. *Mol Ecol* **25**, 5795–5805 (2016).